Current Signature Modeling of Surface-mounted PMSM Drives with Current Sensors Faults

Ciro Attaianese, *Senior Member, IEEE,* Matilde D'Arpino, *Member, IEEE,* Mauro Di Monaco, *Member, IEEE,* and Luigi Pio Di Noia, *Member, IEEE*

***Abstract*—This paper presents the closed-form analytical determination of the current signature of a surface-mounted permanent magnet synchronous motor drive controlled by means of field oriented control strategy, when a fault occurs in one or more current sensors. Both DC offset and gain fault for all phase current sensors are considered. The proposed model includes the response of the control loop and related gains, eliminating the need for phase voltage sensors and complicated state estimation. However, the proposed approach requires the solution of an overdetermined system of equations. Then a new methodology of solution is proposed to save computing time, as an alternative to the classical one based on the Moore-Penrose pseudoinverse matrix. Experimental results and sensitivity analysis to parameter variations confirm the validity of the proposed model.**

***Index Terms*—PMSM drive, current signature, sensor faults.**

I. Introduction

PERMANENT Magnet Synchronous Machines (PMSMs) are widely used in transportation, power generation and other industrial applications thanks to their high power density, precise torque control, large field weakening area and low cooling required for the rotor [1], [2]. PMSMs and the related power electronics can be subjected to several faults due to mechanical, electrical and environmental conditions [3]. In some applications, the continuity of operation is necessary, so an outage in the PMSM drive is unacceptable or may cause great losses. For these reasons, several studies are presented in literature focusing both on early fault detection and on fault-tolerant PMSM drives, to address operations by means of the Predictive Maintenance (PdM) strategies, which consist in estimating the state of health of the drive to decide which maintenance action to perform and when to perform it. To this end, some parameters relating to the state of the drive are constantly monitored to evaluate whether some indicators show signs of a decrease in performance or of incipient failure. One of the techniques used for PdM is Electrical Signature Analysis (ESA) [4]. It is based on the frequency spectra analysis of the electrical signals of the machine at steady-state to find the frequency components whose magnitudes change in the presence of a fault. Thus, the faults can be detected in early stage, and the severity is related to the component magnitude. The advantages of ESA are low intrusiveness, technical and economic viability, and dependence on only the electrical signals of the machine. When the monitored quantities are the motor currents, these methodologies are defined as Motor Current Signature Analysis (MCSA). MCSA has been used extensively to detect specific failure modes in induction motors [5], with reference to static and dynamic rotor eccentricities, broken rotor bars, and bearing failures, together with or as a replacement for thermal and vibrations monitoring that have been used for decades [4]. More recently, researchers have been focused on the use of MCSA for detecting faults in PMSM drives. Several works have been published about MCSA-based methodologies for faults detection in PMSMs. They have approached mainly the detection of open phase fault [6], [7], stator winding inter-turn short circuit [8]–[12], rotor demagnetization [13]–[15], air gap eccentricity [16]–[19]. Obviously, to apply these methods effectively, it is essential to know the effects of faults on the stator current spectrum. This implies the ability to develop a model of the motor and, more generally, of the drive, which takes into account the faults to be detected. Moreover, because a PMSM is always a part of a drive including the control loop as well, the modeling of the current signature corresponding to a fault has to be extended considering the whole drive. From this point of view, particular attention must be paid to current sensors, because they are usually adopted in PMSM drives to generate feedback signals for closed-loop controls, as occurs, for example, with Field Oriented Control (FOC). Therefore, a fault that occurs in a current sensor, in addition to causing a deterioration in the performance of the drive, can modify the current signature generated by other faults, invalidating the effectiveness of the detection. Since the currents available for fault diagnosis are those measured, in this case it would be more appropriate to speak of Drive Current Signature Analysis (DCSA) instead of MCSA. As matter of fact, a closed-form solution of the model of the whole PMSM drive in case of phase current sensor faults is not found in the available literature, probably due to the complexity of the mathematics. To take into account of the control loop, in several of the available references, voltage measurements, together with observers, are often used to diagnose current sensor faults. For example, three Luenberger observers are used in [20] to estimate a fault condition in voltage, current and speed sensors for PMSM. However, for each estimation two set of measurements are required (e.g. voltages and currents

Ciro Attaianese and Luigi Pio Di Noia are with the Department of Electrical Engineering and Information Technology, University of Naples Federico II, via Claudio 21, 80125 Naples, Italy - e-mail: ciro.attaianese@unina.it, luigipio.dinoia@unina.it.

Matilde D'Arpino is with the Department of Mechanical and Aerospace Engineering, Ohio State University, 930 Kinnear Road, Columbus, OH 43212, USA - e-mail: darpino.2@osu.edu.

Mauro Di Monaco is with the Department of Electrical and Information Engineering, University of Cassino and Southern Lazio, via G. Di Biasio 43, 03043 Cassino, Italy - e-mail: mauro.dimonaco@unicas.it.

Manuscript received Xxxxxxx YY, 202Y; revised Xxxxxxx YY, 202Y.

to observe speed and other combination) to cope with the disturbances included in the FOC loop by the fault condition. This increases the number of measurements needed for diagnostic purposes. An equivalent-input-disturbance approach based on integral observer and a fault reconstruction system based on sliding mode observer is proposed in [21], with the ability of differentiating disturbances from faulty conditions for phase current sensor measurements. Voltage measurements are required in this case as well.

The contributions of this paper are as follows. First, it presents the closed-form analytical determination of the current signature of a surface-mounted PMSM drive controlled by means of Field Oriented Control (FOC) strategy, when a fault occurs in one or more current sensors. Both DC offset and gain fault for all phase current sensors are considered, as well as the control loop gains. Second, because the solution of an overdetermined system of equations is required, a new methodology of solution is proposed to save computing time, as an alternative to the classical one based on the Moore-Penrose pseudoinverse matrix. Third, a sensitivity analysis of the proposed solution to the variations of the motor parameters is conducted in detail. The authors had already addressed the problem of modeling the current signature due to current sensor failures in PMSM drives by considering separately offset [22] and gain failures [23], respectively. In this paper, both types of faults are considered to be present simultaneously. Because of the non-linearity of the considered system, the principle of superposition of effects is not applicable, and therefore the structure of the model and the solutions obtained in this paper are significantly different from the ones presented in [22], [23].

The paper is organized as follows. Section II presents a model of a surface-mounted PMSM drive with FOC which allows determining the current signature of the drive by taking into account both current sensor faults and control loop gains. Section III describes how the steady-state closed-form solution of the model can be obtained as solution of an overdetermined system of linear equations. Section IV presents how to solve overdetermined systems of linear equations by means both of the classical Moore-Penrose pseudoinverse matrix and a new methodology which allows saving computing time. In Section V the closed-form analytical solution of the proposed model is given, while Section VI provides its experimental validation. Section VII is devoted to the sensitivity analysis of the proposed model to the variations of the motor parameters. Finally, conclusions and future research directions are given in Section VIII.

II. Drive Model

A Surface-mounted Permanent Magnet Synchronous Motor (SPMSM) fed by a Voltage Source Inverter (VSI) and controlled by means of FOC with Space Vector Modulation (SVM) is here considered and shown in Fig. 1. The mathematical model can be expressed as following [24]

$$\begin{cases} v_{\mathrm{d}} = L\dfrac{\mathrm{d}i_{\mathrm{d}}}{\mathrm{d}t} + Ri_{\mathrm{d}} - p\omega_{\mathrm{r}}Li_{\mathrm{q}} \\ v_{\mathrm{q}} = L\dfrac{\mathrm{d}i_{\mathrm{q}}}{\mathrm{d}t} + Ri_{\mathrm{q}} + p\omega_{\mathrm{r}}Li_{\mathrm{d}} + p\omega_{\mathrm{r}}\phi \end{cases} \tag{1}$$

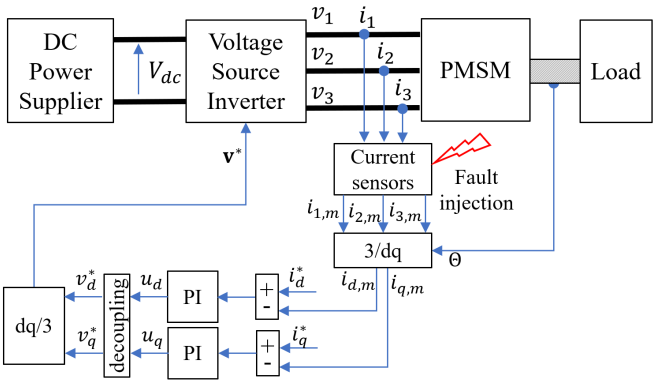

Fig. 1. Schematic of the considered PMSM drive with field oriented control and SVM.

where $v_{\mathrm{d}}, v_{\mathrm{q}}, i_{\mathrm{d}}, i_{\mathrm{q}}$ denote the d- and q-components of motor voltage and current space vectors in the rotor flux reference frame, R and L are the stator resistance and inductance, ω_{r} is the motor speed, p the pole pairs number, ϕ the rotor flux, and t the time.

The voltage inputs $v_{\mathrm{d}}, v_{\mathrm{q}}$ are synthesized by the SVM of the VSI starting from the $\mathbf{v}^*$ space vector defined by the FOC. In detail, on the basis of the desired current space vector components i_{d}^*, i_{q}^*, and of the motor measured current space vector components $i_{\mathrm{d,m}}$, $i_{\mathrm{q,m}}$, the PI controllers calculate the desired electric motor voltage u_d, u_q. A decoupling block is provided to take into account of the cross-coupling terms between d and q-axes, and achieve the components v_{d}^*, v_{q}^* of the VSI voltage reference $\mathbf{v}^*$

$$\begin{cases} v_{\mathrm{d}}^* = k_{\mathrm{Pd}}(i_{\mathrm{d}}^* - i_{\mathrm{d,m}}) + k_{\mathrm{Id}}\int(i_{\mathrm{d}}^* - i_{\mathrm{d,m}})\mathrm{d}t - p\omega_{\mathrm{r}}Li_{\mathrm{q,m}} \\ v_{\mathrm{q}}^* = k_{\mathrm{Pq}}(i_{\mathrm{q}}^* - i_{\mathrm{q,m}}) + k_{\mathrm{Iq}}\int(i_{\mathrm{q}}^* - i_{\mathrm{q,m}})\mathrm{d}t + p\omega_{\mathrm{r}}Li_{\mathrm{d,m}} + p\omega_{\mathrm{r}}\phi \end{cases} \tag{2}$$

where $k_{\mathrm{Pd}}, k_{\mathrm{Pq}}, k_{\mathrm{Id}}, k_{\mathrm{Iq}}$ are the gains of the PI controllers.

Combining (1) and (2) and under the hypothesis that the VSI is ideal (i.e. $v_{\mathrm{d}}^* = v_{\mathrm{d}}$, $v_{\mathrm{q}}^* = v_{\mathrm{q}}$), the model of the PMSM drive becomes

$$\begin{cases} k_{\mathrm{Pd}}(i_{\mathrm{d}}^* - i_{\mathrm{d,m}}) + k_{\mathrm{Id}}\int_0^t (i_{\mathrm{d}}^* - i_{\mathrm{d,m}})\ \mathrm{d}t - p\omega_{\mathrm{r}}Li_{\mathrm{q,m}} \\ \qquad = L\dfrac{\mathrm{d}i_{\mathrm{d}}}{\mathrm{d}t} + Ri_{\mathrm{d}} - p\omega_{\mathrm{r}}Li_{\mathrm{q}} \\ k_{\mathrm{Pq}}(i_{\mathrm{q}}^* - i_{\mathrm{q,m}}) + k_{\mathrm{Iq}}\int_0^t (i_{\mathrm{q}}^* - i_{\mathrm{q,m}})\ \mathrm{d}t + p\omega_{\mathrm{r}}Li_{\mathrm{d,m}} \\ \qquad = L\dfrac{\mathrm{d}i_{\mathrm{q}}}{\mathrm{d}t} + Ri_{\mathrm{q}} + p\omega_{\mathrm{r}}Li_{\mathrm{d}} \end{cases} \tag{3}$$

If all the phase current sensors are healthy, it is

$$i_{\mathrm{d,m}} = i_{\mathrm{d}} \qquad i_{\mathrm{q,m}} = i_{\mathrm{q}} \tag{4}$$

and the solution of (3) allows determining the current components i_{d} and i_{q} provided that the motor speed is known and constant. When a fault occurs in the sensor of the h-th phase current, the measured current $i_{h,\mathrm{m}}$, and the actual current i_h will be different, i.e.

$$i_{h,\mathrm{m}} = k_h i_h + \Delta_h \qquad \text{with } h = 1, 2, 3 \tag{5}$$

where k_h and Δ_h represent the gain and the offset of the h-th current sensor, respectively. Obviously, if $\Delta_h = 0$ and $k_h = 1$,

the sensor is healthy. When a sensor current fault occurs, to model the drive according to (3), the d- and q-components of the measured currents, $i_{\mathrm{d,m}}$ and $i_{\mathrm{q,m}}$, have to be determined as a function of i_{d} and i_{q}.

Denoting with $\mathbf{i}$ and $\mathbf{i}_{\mathrm{m}}$ the space vectors of the actual and of the measured motor current, with the subscripts α and β the vector coordinates in the stator reference frame, it results

$$\mathbf{i} = \frac{2}{3}\sum_{h=1}^{3} i_h \, \mathrm{e}^{\frac{2\pi}{3}(h-1)} = i_\alpha + \mathrm{j} i_\beta \tag{6}$$

$$\mathbf{i}_{\mathrm{m}} = \boldsymbol{\delta} + \frac{2}{3}\sum_{h=1}^{3} k_h i_h \, \mathrm{e}^{\frac{2\pi}{3}(h-1)} = i_{\alpha,\mathrm{m}} + \mathrm{j} i_{\beta,\mathrm{m}} \tag{7}$$

where

$$\boldsymbol{\delta} = \frac{2}{3}\sum_{h=1}^{3} \Delta_h \, \mathrm{e}^{\frac{2\pi}{3}(h-1)} = \delta_\alpha + \mathrm{j}\delta_\beta \tag{8}$$

Since it is

$$i_1 + i_2 + i_3 = 0 \tag{9}$$

then from (6) we obtain

$$\begin{cases} i_1 = i_\alpha \\ i_2 = -\dfrac{1}{2} i_\alpha + \dfrac{\sqrt{3}}{2} i_\beta \\ i_2 = -\dfrac{1}{2} i_\alpha - \dfrac{\sqrt{3}}{2} i_\beta \end{cases} \tag{10}$$

and substituting (10) and (8) in (7) yields

$$\begin{cases} i_{\alpha,\mathrm{m}} = \dfrac{4k_1 + k_2 + k_3}{6} i_\alpha - \dfrac{k_2 - k_3}{2\sqrt{3}} i_\beta + \delta_\alpha \\ i_{\beta,\mathrm{m}} = \dfrac{k_3 - k_2}{2\sqrt{3}} i_\alpha + \dfrac{k_2 + k_3}{2} i_\beta + \delta_\beta \end{cases} \tag{11}$$

Considering that the d- and q-axes components of the space vectors $\mathbf{i}$ and $\mathbf{i}_{\mathrm{m}}$ are given by

$$i_{\mathrm{d}} + \mathrm{j} i_{\mathrm{q}} = \mathbf{i}\, \mathrm{e}^{-\mathrm{j}p\theta}; \qquad i_{\mathrm{d,m}} + \mathrm{j} i_{\mathrm{q},,\mathrm{m}} = \mathbf{i}_{\mathrm{m}}\, \mathrm{e}^{-\mathrm{j}p\theta} \tag{12}$$

where θ is the rotor position, combining (11) and (12) yields

$$\begin{cases} i_{\mathrm{d,m}} = \big(w_1 + s\big) i_{\mathrm{d}} + w_2 i_{\mathrm{q}} + \delta_\alpha \cos p\theta + \delta_\beta \sin p\theta \\ i_{\mathrm{q,m}} = w_2 i_{\mathrm{d}} - \big(w_1 - s\big) i_{\mathrm{q}} - \delta_\alpha \sin p\theta + \delta_\beta \cos p\theta \end{cases} \tag{13}$$

with

$$\begin{cases} w_1 = q\cos 2p\theta + r \sin 2p\theta \\ w_2 = r\cos 2p\theta - q \sin 2p\theta \end{cases} \tag{14}$$

and

$$q = \frac{2k_1 - k_2 - k_3}{6}; \quad r = \frac{\sqrt{3}(k_3 - k_2)}{6}; \quad s = \frac{k_1 + k_2 + k_3}{3} \tag{15}$$

Equation (13) allows expressing $i_{\mathrm{d,m}}$ and $i_{\mathrm{q,m}}$ as a function of i_{d} and i_{q}, without the need of direct measurement or estimation of the motor voltage. If constant speed is assumed, i.e.

$$\theta(t) = \omega_{\mathrm{r}} t \tag{16}$$

substituting (13) in (3) and taking the derivative gives

$$\begin{cases} L\dfrac{\mathrm{d}i_{\mathrm{d}}^2}{\mathrm{d}t^2} + z_1 \dfrac{\mathrm{d}i_{\mathrm{d}}}{\mathrm{d}t} + z_2 \dfrac{\mathrm{d}i_{\mathrm{q}}}{\mathrm{d}t} + z_3 i_{\mathrm{d}} + z_4 i_{\mathrm{q}} + z_5 = k_{\mathrm{id}} i_{\mathrm{d}}^* \\ L\dfrac{\mathrm{d}i_{\mathrm{q}}^2}{\mathrm{d}t^2} + y_1 \dfrac{\mathrm{d}i_{\mathrm{d}}}{\mathrm{d}t} + y_2 \dfrac{\mathrm{d}i_{\mathrm{q}}}{\mathrm{d}t} + y_3 i_{\mathrm{d}} + y_4 i_{\mathrm{q}} + y_5 = k_{\mathrm{iq}} i_{\mathrm{q}}^* \end{cases} \tag{17}$$

where

$$\begin{cases} z_1 = R + (w_1 + s)k_{\mathrm{pd}} + w_2 p\omega_{\mathrm{r}} L \\ z_2 = w_2 k_{\mathrm{pd}} - (w_1 - s + 1)p\omega_{\mathrm{r}} L \\ z_3 = 2w_2 p\omega_{\mathrm{r}} k_{\mathrm{pd}} - 2w_1 p^2 \omega_{\mathrm{r}}^2 L + (w_1 + s)k_{\mathrm{id}} \\ z_4 = -2w_1 p\omega_{\mathrm{r}} k_{\mathrm{pd}} - w_2(2p^2\omega_{\mathrm{r}}^2 L - k_{\mathrm{id}}) \\ z_5 = \delta_\alpha\big[(k_{\mathrm{id}} - p^2\omega_{\mathrm{r}}^2 L)\cos p\theta - k_{\mathrm{pd}} p\omega_{\mathrm{r}} \sin p\theta\big] \\ \quad\; + \delta_\beta\big[k_{\mathrm{pd}} p\omega_{\mathrm{r}} \cos p\theta + (k_{\mathrm{id}} - p^2\omega_{\mathrm{r}}^2 L)\sin p\theta\big] \\ y_1 = w_2 k_{\mathrm{pq}} - (w_1 + s - 1)p\omega_{\mathrm{r}} L \\ y_2 = R - (w_1 - s)k_{\mathrm{pq}} - w_2 p\omega_{\mathrm{r}} L \\ y_3 = -2w_1 p\omega_{\mathrm{r}} k_{\mathrm{pq}} - w_2(2p^2\omega_{\mathrm{r}}^2 L - k_{\mathrm{iq}}) \\ y_4 = -2w_2 p\omega_{\mathrm{r}} k_{\mathrm{pq}} + 2w_1 p^2 \omega_{\mathrm{r}}^2 L - (w_1 - s)k_{\mathrm{iq}} \\ y_5 = \delta_\alpha\big[-(k_{\mathrm{iq}} - p^2\omega_{\mathrm{r}}^2 L)\sin p\theta - k_{\mathrm{pq}} p\omega_{\mathrm{r}} \cos p\theta\big] \\ \quad\; - \delta_\beta\big[(k_{\mathrm{iq}} - p^2\omega_{\mathrm{r}}^2 L)\cos p\theta + k_{\mathrm{pq}} p\omega_{\mathrm{r}} \sin p\theta\big] \end{cases} \tag{18}$$

The proposed model does not need knowledge of the input voltage to the electric machine to assess the impact of current sensor faults, since the response of the FOC loop is included. The set of equations in (17) correlates the actual electric machine currents to the measured ones and the current sensors fault conditions. As matter of fact, the gains k_h are included in the factors q, r, s, while the offsets Δ_h appear in factors z_5, y_5. Note that the effects of gain and offset errors cannot be decoupled when they occur simultaneously.

III. Steady-state solution

Assuming that the inverter modulation is ideal, the solution of (17) allows to analytically determine the current components i_{d} and i_{q} for any value of the gains k_1, k_2, k_3, and of the offsets Δ_1, Δ_2, Δ_3 of the current sensors, taking into account the whole control loop. As could easily be expected, despite the presence of the decoupling block in the control loop, the two equations of the system (17) are no longer decoupled when a gain fault of one or more phase current sensors occurs, because in (17) it is $z_2 \neq 0$, $z_4 \neq 0$, and $y_1 \neq 0$, $y_3 \neq 0$. For determining the steady-state solution of the system (17) in analytical closed-form, the method of undetermined coefficients can be used [25]. Thus, the steady-state solution has the form

$$\begin{cases} i_{\mathrm{d}}(t) = \displaystyle\sum_{h=1}^{n} \big[a_{\mathrm{d},h}\cos(hp\omega_r t) + b_{\mathrm{d},h}\sin(hp\omega_r t)\big] + c_{\mathrm{d}} \\ i_{\mathrm{q}}(t) = \displaystyle\sum_{h=1}^{n} \big[a_{\mathrm{q},h}\cos(hp\omega_r t) + b_{\mathrm{q},h}\sin(hp\omega_r t)\big] + c_{\mathrm{q}} \end{cases} \tag{19}$$

with

$$\begin{cases} \lim\limits_{h\to\infty} a_{\mathrm{d},h} = 0; & \lim\limits_{h\to\infty} b_{\mathrm{d},h} = 0 \\ \lim\limits_{h\to\infty} a_{\mathrm{q},h} = 0; & \lim\limits_{h\to\infty} b_{\mathrm{q},h} = 0 \end{cases} \tag{20}$$

From (13), (14) and (17), it is possible to deduce that, when a fault of one or more current sensors occurs, the steady-state i_{d} and i_{q} are given by the sum of a series of harmonics having angular frequency $hp\omega_{\mathrm{r}}$, with h integer. In particular, if only a gain fault occurs, only the harmonics corresponding to even values of h are present [23], while if only an offset fault occurs there are only the harmonics corresponding to odd values of h [22]. The coefficients $a_{\mathrm{d},h}$, $b_{\mathrm{d},h}$, $a_{\mathrm{q},h}$, $b_{\mathrm{q},h}$, c_{d}, c_{q} are functions of motor parameters, motor speed, gains of the control loops, gains and offsets of the phase current sensors. These coefficients must be determined in such a way that the currents i_{d} and i_{q} given by (19) are solutions of system (17). Imposing this condition, the following relations can be achieved

$$\begin{cases} \sum_{k=1}^{n+2} \left[f_{\mathrm{d},k} \cos(pk\omega_{\mathrm{r}}t) + g_{\mathrm{d},k} \sin(pk\omega_{\mathrm{r}}t) \right] + f_{d,0} = k_{\mathrm{id}} i_{\mathrm{d}}^* \\ \sum_{k=1}^{n+2} \left[f_{\mathrm{q},k} \cos(pk\omega_{\mathrm{r}}t) + g_{\mathrm{q},k} \sin(pk\omega_{\mathrm{r}}t) \right] + f_{q,0} = k_{\mathrm{iq}} i_{\mathrm{q}}^* \end{cases} \tag{21}$$

where $f_{\mathrm{d},0}$, $f_{\mathrm{q},0}$, $f_{\mathrm{d},k}$, $g_{\mathrm{d},k}$, $f_{\mathrm{q},k}$, $g_{\mathrm{q},k}$ are linear functions of the coefficients $a_{\mathrm{d},h}$, $b_{\mathrm{d},h}$, $a_{\mathrm{q},h}$, $b_{\mathrm{q},h}$, c_{d}, c_{q}, which have to be determined by solving the following system of linear equations

$$\begin{cases} f_{\mathrm{d},0}\left(a_{\mathrm{d},h}, b_{\mathrm{d},h}, a_{\mathrm{q},h}, b_{\mathrm{q},h}, c_{\mathrm{d}}, c_{\mathrm{q}}\right) = k_{\mathrm{id}} i_{\mathrm{d}}^* \\ f_{\mathrm{d},1}\left(a_{\mathrm{d},h}, b_{\mathrm{d},h}, a_{\mathrm{q},h}, b_{\mathrm{q},h}, c_{\mathrm{d}}, c_{\mathrm{q}}\right) = \\ \qquad = \delta_\alpha (p^2 \omega_{\mathrm{r}}^2 L - k_{\mathrm{id}}) - \delta_\beta \, p\omega_{\mathrm{r}} k_{\mathrm{pd}} \\ f_{\mathrm{d},k}\left(a_{\mathrm{d},h}, b_{\mathrm{d},h}, a_{\mathrm{q},h}, b_{\mathrm{q},h}, c_{\mathrm{d}}, c_{\mathrm{q}}\right) = 0 \\ g_{\mathrm{d},1}\left(a_{\mathrm{d},h}, b_{\mathrm{d},h}, a_{\mathrm{q},h}, b_{\mathrm{q},h}, c_{\mathrm{d}}, c_{\mathrm{q}}\right) = \\ \qquad = \delta_\alpha p\omega_{\mathrm{r}} k_{\mathrm{pd}} + \delta_\beta (p^2 \omega_{\mathrm{r}}^2 L - k_{\mathrm{id}}) \\ g_{\mathrm{d},k}\left(a_{\mathrm{d},h}, b_{\mathrm{d},h}, a_{\mathrm{q},h}, b_{\mathrm{q},h}, c_{\mathrm{d}}, c_{\mathrm{q}}\right) = 0 \\ f_{\mathrm{q},0}\left(a_{\mathrm{d},h}, b_{\mathrm{d},h}, a_{\mathrm{q},h}, b_{\mathrm{q},h}, c_{\mathrm{d}}, c_{\mathrm{q}}\right) = k_{\mathrm{iq}} i_{\mathrm{q}}^* \\ f_{\mathrm{q},1}\left(a_{\mathrm{d},h}, b_{\mathrm{d},h}, a_{\mathrm{q},h}, b_{\mathrm{q},h}, c_{\mathrm{d}}, c_{\mathrm{q}}\right) = \\ \qquad = \delta_\alpha p\omega_{\mathrm{r}} k_{\mathrm{pq}} + \delta_\beta (p^2 \omega_{\mathrm{r}}^2 L - k_{\mathrm{iq}}) \\ f_{\mathrm{q},k}\left(a_{\mathrm{d},h}, b_{\mathrm{d},h}, a_{\mathrm{q},h}, b_{\mathrm{q},h}, c_{\mathrm{d}}, c_{\mathrm{q}}\right) = 0 \\ g_{\mathrm{q},1}\left(a_{\mathrm{d},h}, b_{\mathrm{d},h}, a_{\mathrm{q},h}, b_{\mathrm{q},h}, c_{\mathrm{d}}, c_{\mathrm{q}}\right) = \\ \qquad = \delta_\alpha (k_{\mathrm{iq}} - p^2 \omega_{\mathrm{r}}^2 L) + \delta_\beta \, p\omega_{\mathrm{r}} k_{\mathrm{pq}} \\ g_{\mathrm{q},k}\left(a_{\mathrm{d},h}, b_{\mathrm{d},h}, a_{\mathrm{q},h}, b_{\mathrm{q},h}, c_{\mathrm{d}}, c_{\mathrm{q}}\right) = 0 \end{cases} \tag{22}$$

with $h \in \{1, \ldots, n\}$ and $k \in \{2, \ldots, (n+2)\}$. The analytical expressions of the functions $f_{\mathrm{d},0}$, $f_{\mathrm{q},0}$, $f_{\mathrm{d},1}$, $g_{\mathrm{d},1}$, $f_{\mathrm{d},k}$, $g_{\mathrm{d},k}$, $f_{\mathrm{q},1}$, $g_{\mathrm{q},1}$, $f_{\mathrm{q},k}$, $g_{\mathrm{q},k}$ are given in the Appendix.

Because in (22) the number of equations, $(4n + 10)$, is greater than the number of unknowns, $(4n + 2)$, it is an overdetermined system of linear equations. In the following section, a short overview of how to solve such a system is given.

IV. Solution of Overdetermined Systems of Linear Equations: A Short Overview

Let us consider a system of linear equations written in matrix form as

$$\mathbf{A}\mathbf{x} = \mathbf{b} \tag{23}$$

where $\mathbf{A}$ is the $m \times n$ coefficient matrix, $\mathbf{x}$ the $n-$dimensional vector of unknowns, and $\mathbf{b}$ the $m-$dimensional vector of constants. In the case of overdetermined systems, it is $m > n$. Assuming that $\mathrm{rank}(\mathbf{A}) = n$ and the number of linearly independent equations is greater than the number of unknowns, the rank of the augmented matrix is $(n + 1)$ and an exact solution cannot be found, since there is no vector of unknowns $\mathbf{x}$ which simultaneously satisfy all the equations of (23). However, it is always possible to find the best approximate solution, which means to find a vector $\mathbf{x}^*$ in such a way that $\mathbf{A}\mathbf{x}^*$ is as close to $\mathbf{b}$ as possible. If we set

$$\mathbf{A} = [a_{i,j}] \quad \mathbf{x} = [x_j] \quad \mathbf{b} = [b_i] \tag{24}$$

with $i \in \{1, \ldots, m\}$ and $j \in \{1, \ldots, n\}$, then the error, or residual, r_i corresponding to the $i-$th equation is:

$$r_i = b_i - \sum_{j=1}^{n} a_{i.j} x_j \tag{25}$$

and an error vector $\mathbf{r}$ can be defined as

$$\mathbf{r} = \begin{bmatrix} r_1 \\ r_2 \\ \vdots \\ r_m \end{bmatrix} = \mathbf{b} - \mathbf{A}\mathbf{x} \tag{26}$$

The solution $\mathbf{x}^*$ of (23) which minimizes the sum of squared errors $\varphi(\mathbf{x})$

$$\varphi(\mathbf{x}) = \sum_{i=1}^{m} r_i^2 = \mathbf{r}^T \mathbf{r} \tag{27}$$

is given by

$$\mathbf{x}^* = (\mathbf{A}^{\mathrm{T}}\mathbf{A})^{-1}\mathbf{A}^{\mathrm{T}}\mathbf{b} = \mathbf{A}^{\dagger}\mathbf{b} \tag{28}$$

The matrix $\mathbf{A}^{\dagger}$ is known as Moore-Penrose inverse of matrix $\mathbf{A}$, or simply pseeudoinverse of $\mathbf{A}$ [26]. In practice, the determination of the pseudoinverse matrix is not easy to compute by hand, even if n and m are small. Therefore, the use of dedicated subroutines is mandatory. In Matlab®, the subroutine for calculating the pseudoinverse is based on the Singular Value Decomposition (SVD) algorithm. However, a long computing time could be required, which may be critical especially in real time applications, such as the detection, isolation and estimation of fault conditions. Furthermore, numeric stability problems could occur when the elements of the $\mathbf{A}$ matrix are very small or very different from each other.

For these reasons, an alternative solution is proposed in this paper, that allows both to reduce computing times and to avoid numerical stability problems. It consists in partitioning the matrix $\mathbf{A}$ into two submatrices, $\mathbf{A}'$ and $\mathbf{A}''$, having size $n \times n$ and $(m - n) \times n$, respectively

$$\mathbf{A} = \begin{bmatrix} \mathbf{A}' \\ \mathbf{A}'' \end{bmatrix} \tag{29}$$

In this way, system (23) can be rewritten as the union of two sub-systems

$$\mathbf{A}'\mathbf{x} = \mathbf{b}' \tag{30}$$

$$\mathbf{A}''\mathbf{x} = \mathbf{b}'' \tag{31}$$

where the vectors $\mathbf{b}'$, $\mathbf{b}''$ are the sub-vectors of $\mathbf{b}$ corresponding to submatrices $\mathbf{A}'$, $\mathbf{A}''$, and have size n and $(m - n)$, respectively. Any solution of system (23), if exists, is also

solution of these two sub-systems and vice versa. If the ranks of $\mathbf{A}'$ and of the correspondent augmented matrix are n and $(n+1)$, respectively, then system (30) is consistent and its solution is unique

$$\mathbf{x}^* = (\mathbf{A}')^{-1}\mathbf{b}' \tag{32}$$

while system (31) has no solution, and therefore is not satisfied by $\mathbf{x}^*$.

Let's assume, without loss of generality, that $\mathbf{A}'$ is composed by the first n rows of $\mathbf{A}$ and let $\mathbf{x}^*$ be the solution of the first sub-system (30). Thus, in this case the error vector $\mathbf{r}$ is

$$\mathbf{r} = \begin{bmatrix} 0 \\ 0 \\ \vdots \\ 0 \\ r_{n+1} \\ r_{n+2} \\ \vdots \\ r_m \end{bmatrix} = \mathbf{b} - \mathbf{A}\mathbf{x}^* \tag{33}$$

and the sum of squared errors $\varphi(\mathbf{x}^*)$ is given by

$$\varphi(\mathbf{x}^*) = \sum_{i=n+1}^{m} r_i^2 \tag{34}$$

Thus, $\mathbf{x}^*$ can be regarded as an approximate solution of system (23) which gives rise to a total squared error defined by (34). In this way, the computation of the pseudoinverse of the matrix $\mathbf{A}$ is not required, and this results in a reduction of the calculation time by at least an order of magnitude. Obviously, the validity of the proposed method of solution of overdetermined system (23) depends on the structure of the matrices $\mathbf{A}'$ and $\mathbf{A}''$ and on the residuals generated by the found solution. In particular, a better approximation of the solution is achieved when the less significant are the equations corresponding to the matrix $\mathbf{A}''$. Hence, a proper preliminary determination of the system (30) to be solved is required.

V. Closed-form analytical solution

In the considered case of (22), the system matrix $\mathbf{A}$ is a $(4n+10)\times(4n+2)$ matrix, and

$$\boldsymbol{x}^{\mathrm{T}} = \big[\underbrace{a_{\mathrm{d},h} \quad b_{\mathrm{d},h} \quad a_{\mathrm{q},h} \quad b_{\mathrm{q},h}}_{h=1,\ldots,n} \quad c_{\mathrm{d}} \quad c_{\mathrm{q}}\big] \tag{35}$$

while the vector of constants $\mathbf{b}$ can be easily deduced from (22).

According to the method of solution proposed in Section IV, to solve the system of linear equations (23), a new system matrix $\mathbf{A}'$ has to be considered, which must be a square submatrix of the matrix $\mathbf{A}$, having order $(4n+2)\times(4n+2)$, chosen in such a way that its rank is $(4n+2)$. It is immediate to verify that the sub-system of equations of system (22) obtained

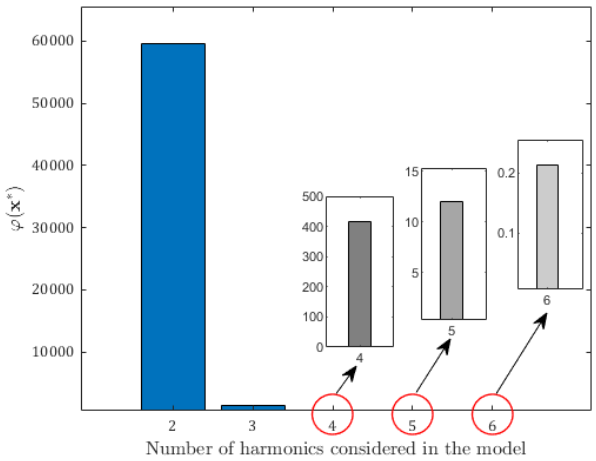

Fig. 2. Calculation of residual for different number of harmonics considered in the model.

for $k = n+1$ is homogeneous and contains only the unknowns $a_{\mathrm{d},n-1}$, $b_{\mathrm{d},n-1}$, $a_{\mathrm{q},n-1}$, $b_{\mathrm{q},n-1}$, i.e.

$$\begin{cases} f_{\mathrm{d},n+1}\left(a_{\mathrm{d},n-1}, b_{\mathrm{d},n-1}, a_{\mathrm{q},n-1}, b_{\mathrm{q},n-1}\right) = 0 \\ g_{\mathrm{d},n+1}\left(a_{\mathrm{d},n-1}, b_{\mathrm{d},n-1}, a_{\mathrm{q},n-1}, b_{\mathrm{q},n-1}\right) = 0 \\ f_{\mathrm{q},n+1}\left(a_{\mathrm{d},n-1}, b_{\mathrm{d},n-1}, a_{\mathrm{q},n-1}, b_{\mathrm{q},n-1}\right) = 0 \\ g_{\mathrm{q},n+1}\left(a_{\mathrm{d},n-1}, b_{\mathrm{d},n-1}, a_{\mathrm{q},n-1}, b_{\mathrm{q},n-1}\right) = 0 \end{cases} \tag{36}$$

while the sub-system of equations obtained for $k = n+2$ is homogeneous and contains only the unknowns $a_{\mathrm{d},n}$, $b_{\mathrm{d},n}$, $a_{\mathrm{q},n}$, $b_{\mathrm{q},n}$,

$$\begin{cases} f_{\mathrm{d},n+2}\left(a_{\mathrm{d},n}, b_{\mathrm{d},n}, a_{\mathrm{q},n}, b_{\mathrm{q},n}\right) = 0 \\ g_{\mathrm{d},n+2}\left(a_{\mathrm{d},n}, b_{\mathrm{d},n}, a_{\mathrm{q},n}, b_{\mathrm{q},n}\right) = 0 \\ f_{\mathrm{q},n+2}\left(a_{\mathrm{d},n}, b_{\mathrm{d},n}, a_{\mathrm{q},n}, b_{\mathrm{q},n}\right) = 0 \\ g_{\mathrm{q},n+2}\left(a_{\mathrm{d},n}, b_{\mathrm{d},n}, a_{\mathrm{q},n}, b_{\mathrm{q},n}\right) = 0 \end{cases} \tag{37}$$

Both the equations of sub-systems (36) and (37) are linearly dependent, because the rank of the corresponding coefficient matrices is always equal to two. Moreover, due to (20) these equations can be regarded as the least significant ones of system (22). Therefore, we can assume as matrix $\mathbf{A}'$ and vector $\mathbf{b}'$ the ones obtained eliminating the equations (36) and (37) from system (22). Thus, an approximated solution $\mathbf{x}^*$ of (22) is given by

$$\mathbf{x}^* = \left(\mathbf{A}'\right)^{-1}\mathbf{b}' \tag{38}$$

As regards the choice of n, i.e. the number of terms to be considered for the analytical determination of the currents i_{d} and i_{q} expressed by (19), it should be noted that if the two PI controllers are the same ($k_{\mathrm{pd}} = k_{\mathrm{pq}}; k_{\mathrm{id}} = k_{\mathrm{iq}}$) the exact solution of equations (17) is obtained for $n = 2$, i.e. the d-q current components contain only the first two harmonics, having angular frequency $p\omega_{\mathrm{r}}$ and $2p\omega_{\mathrm{r}}$, respectively.

In the most general case, i.e. when $k_{\mathrm{pd}} \neq k_{\mathrm{pq}}; k_{\mathrm{id}} \neq k_{\mathrm{iq}}$, the solution of (38) is better approximated as greater is the value of n in (19). The degree of approximation of the solution $\mathbf{x}^*$ found for a given value of n is just given by the value of the sum of squared residuals $\varphi(\mathbf{x}^*)$ defined by (34).

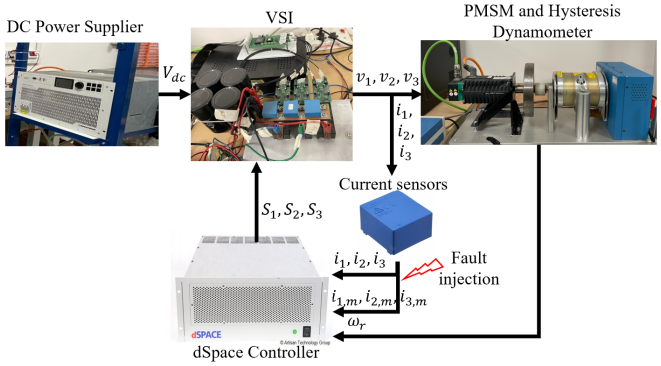

Fig. 3. Experimental setup.

TABLE I
PARAMETERS OF THE PMSM DRIVE

Rated power	1.23	kW
Rated torque	3.9	Nm
Rated speed	blue3000	rpm
Rated current (rms)	2.7	A
Pole pairs	3	
Stator resistance	3.7	Ω
Stator inductance	0.012	H
Rotor flux	0.27	Wb
Total inertia	0.0603	kg m^2
DC-link voltage	400	V
$k_{\mathrm{Pd}}, k_{\mathrm{Id}}, k_{\mathrm{Pq}}, k_{\mathrm{Iq}}$	39, 9, 20, 10	

As an example, Fig.2 shows the residual calculated for a different number of harmonics considered in the model. The values are obtained using the parameters of the drives reported in Table I, operating at 1000 rpm, and with a load torque of 1.15 Nm. As it is well highlighted by the trends of the residuals, $\varphi(\mathbf{x}^*)$ is negligible when the number of harmonics considered in the model is bigger than 5. Similar results are obtained in other operating conditions.

VI. EXPERIMENTAL VALIDATION

The drive shown in Fig. 3 is realized in a laboratory environment using a 1.23 kW three-phase surface-mounted PMSM from Control Technique Unimotor (Model 95UMB300CACAA), a two-level three-phase VSI based on Mitsubishi PM100DSA120IP, and a hysteresis dynamometer from Magtrol (Model HD-715-8NA). The parameters of the system are given in Table I. The electric drive is controlled using a FOC for which the input is the torque reference. The controller is implemented on a dSPACE modular system based on DS1006 processor board, while the symmetric modulation technique is implemented on an Altera CPLD EPM7160SLC84 platform. The FOC loop and modulation technique are synchronized with an interrupt of 100 μs. The three phase currents are measured by LEM Current Transducers LA 25-NP and the sensor current faults are artificially generated by adding offsets and gains in the dSPACE platform. In this way, both measured and real motor currents are available in this experimental set up, as shown in Fig. 3, allowing for an accurate verification of the performance of the proposed modeling approach.

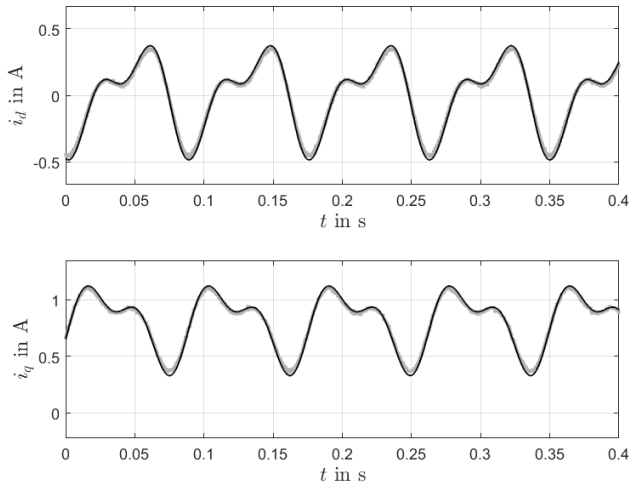

Fig. 4. Comparison between the experimental i_d and i_q currents (gray lines) and the model results (black lines): load of 1.15 Nm; speed of 200 rpm; (k_1, k_2, k_3)=(1, 2, 1); $(\Delta_1, \Delta_2, \Delta_3)$=(0.3, -0.4, 0.5)A.

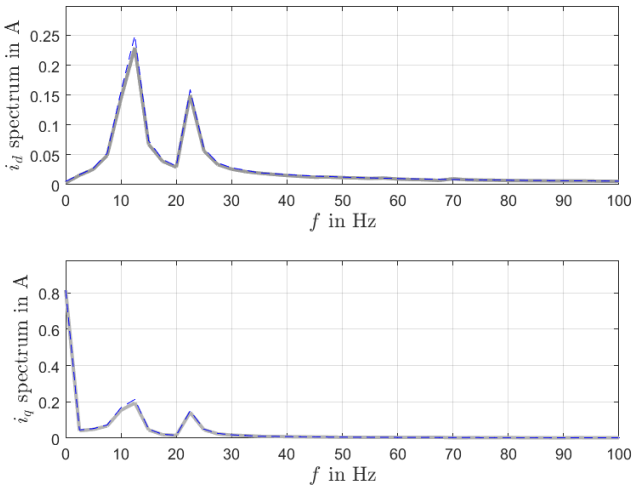

Fig. 5. FFT spectra of the experimental i_d and i_q currents (gray lines) and the model results (blue lines): load of 1.15 Nm; speed of 200 rpm; (k_1, k_2, k_3)=(1, 2, 1); $(\Delta_1, \Delta_2, \Delta_3)$=(0.3, -0.4, 0.5)A.

The experimental validation of the proposed model has been carried out considering the model with $n = 6$ harmonics and the experimental setup at different values of load torque, speed, current sensors gain faults and offsets. As an example, Fig. 4, 6, 8 show the experimental and the calculated $d-$ and $q-$ axis motor currents in some of the considered operating conditions, while Fig. 5, 7, 9 show the corresponding FFT spectra. The proposed model has been also experimentally verified when only the offset faults or the gain faults occur in the phase current sensors. Some results are shown in Figs. 10, 11, (only offset fault), and Fig.s 12, 13 (only gain fault). As it is highlighted by the results, there is an excellent match between the experimental trends and the model results. The proposed model is always able to capture and properly estimate the current harmonic content due to the offset and

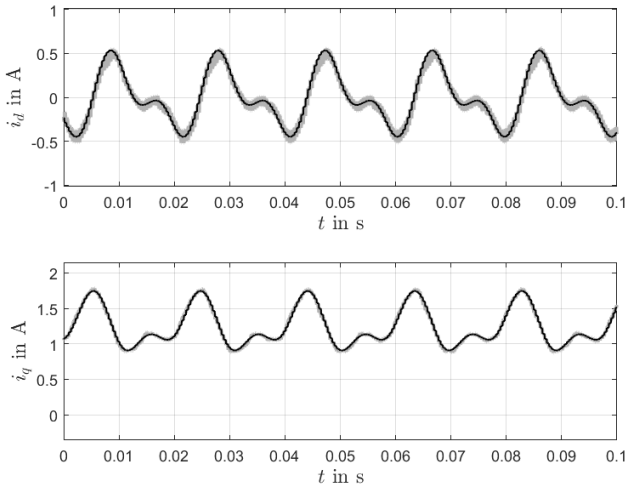

Fig. 6. Comparison between the experimental i_d and i_q currents (gray lines) and the model results (black lines): load of 1.15 Nm; speed of 1000 rpm; (k_1, k_2, k_3)=(1, 2, 1); $(\Delta_1, \Delta_2, \Delta_3)$=(0.3, -0.4, 0.5)A.

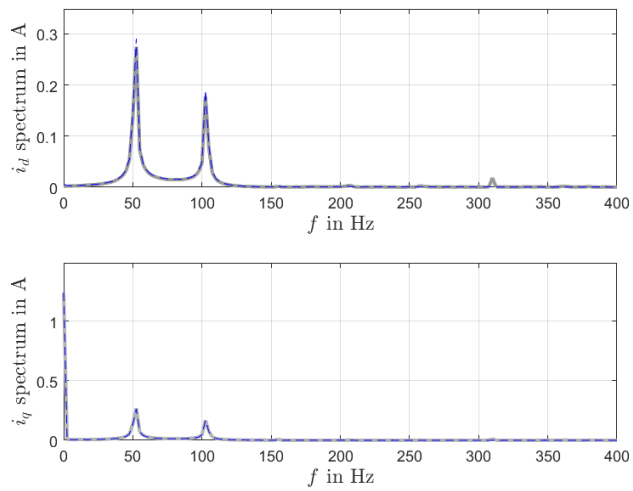

Fig. 7. FFT spectra of the experimental i_d and i_q currents (gray lines) and the model results (blue lines): load of 1.15 Nm; speed of 1000 rpm; (k_1, k_2, k_3)=(1, 2, 1); $(\Delta_1, \Delta_2, \Delta_3)$=(0.3, -0.4, 0.5)A.

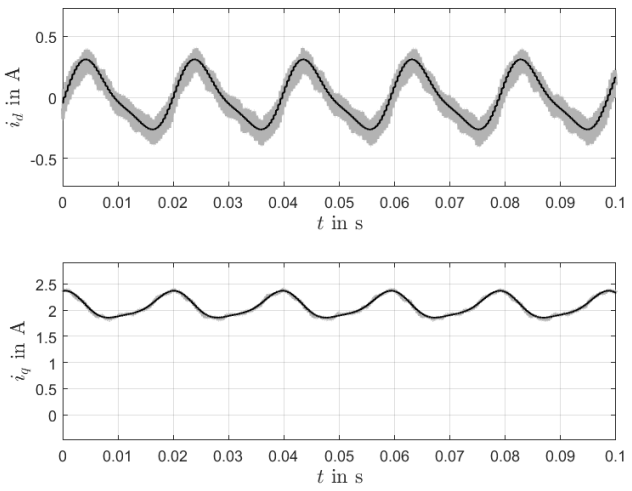

Fig. 8. Comparison between the experimental i_d and i_q currents (grey lines) and the model results (black lines): load of 2.3 Nm; speed of 1000 rpm; (k_1, k_2, k_3)=(1, 2, 1); $(\Delta_1, \Delta_2, \Delta_3)$=(0.3, -0.4, 0.5)A.

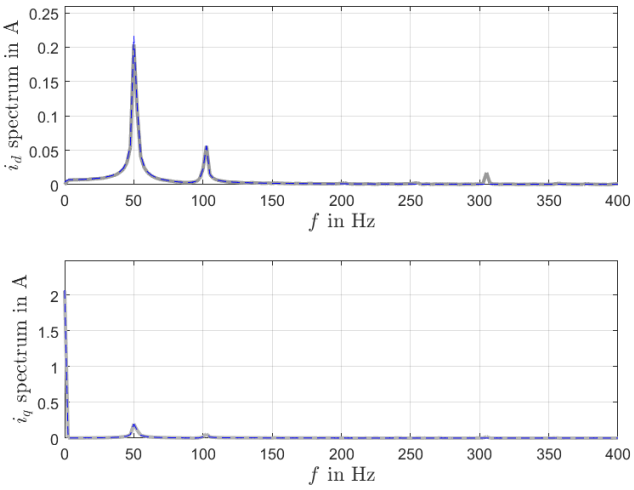

Fig. 9. FFT spectra of the experimental i_d and i_q currents (grey lines) and the model results (blue lines): load of 2.3 Nm; speed of 1000 rpm; (k_1, k_2, k_3)=(1, 2, 1); $(\Delta_1, \Delta_2, \Delta_3)$=(0.3, -0.4, 0.5)A.

gain faults. Other operating conditions have been analyzed and not reported in the paper for lack of space, always obtaining a root-mean-square error less than 5.3%.

VII. Sensitivity Analysis

The sensitivity analysis of a model to the variations of the parameters on which it depends represents one of the crucial points to assess the validity of the model for its usability. Of course the resistance and the inductance values of the motor can be calibrated by performing proper tests, but in any case they will vary with the variation of the operating temperature, the speed and the aging of the motor. From the theoretical point of view, we can express by means of first-order Taylor series approximation the variation $\Delta\mathbf{x}$ of the solution $\mathbf{x}^*$ of the model corresponding to an arbitrary variation Δp_i of the model parameter p_i:

$$\Delta\mathbf{x} \approx \left.\frac{\partial \mathbf{x}}{\partial p_i}\right|_{\mathbf{x}^*} \Delta p_i \tag{39}$$

where the subscript $\mathbf{x}^*$ indicates the point where derivative is calculated.

Therefore, the partial derivative of the vector $\mathbf{x}$ with respect to a parameter p_i, calculated at a given point $\mathbf{x}^*$, can be taken as a measure of the sensitivity of $\mathbf{x}$ with respect to the variations of p_i at the point $\mathbf{x}^*$. From (38):

$$\frac{\partial \mathbf{x}}{\partial p_i} = \frac{\partial}{\partial p_i}\left[(\mathbf{A}')^{-1}\,\mathbf{b}'\right] = \frac{\partial (\mathbf{A}')^{-1}}{\partial p_i}\mathbf{b}' + (\mathbf{A}')^{-1}\frac{\partial \mathbf{b}'}{\partial p_i} \tag{40}$$

Because

$$\mathbf{A}'(\mathbf{A}')^{-1} = \mathbf{I} \tag{41}$$

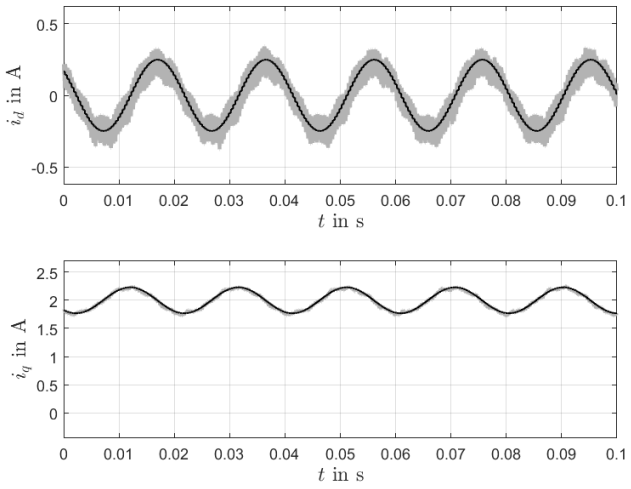

Fig. 10. Comparison between the experimental i_d and i_q currents (grey lines) and the model results (black lines): load of 2.3 Nm; speed of 1000 rpm; (k_1, k_2, k_3)=(1, 1, 1); $(\Delta_1, \Delta_2, \Delta_3)$=(0.3, -0.4, 0.5)A.

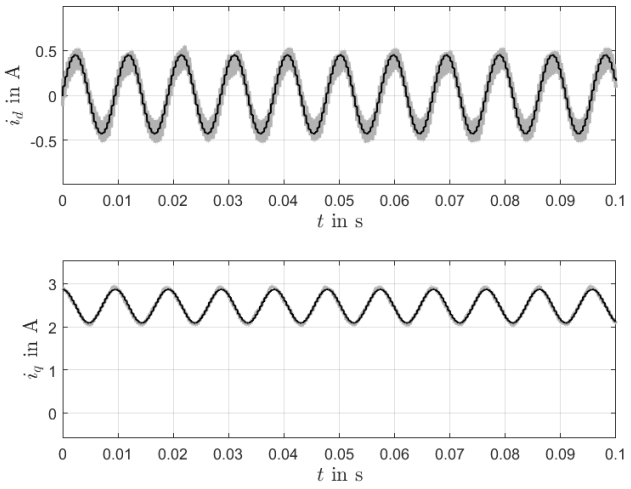

Fig. 12. Comparison between the experimental i_d and i_q currents (grey lines) and the model results (black lines): load of 2.3 Nm; speed of 1000 rpm; current sensors gains (k_1, k_2, k_3)=(1, 0.5, 1);$(\Delta_1, \Delta_2, \Delta_3)$=(0, 0, 0)A.

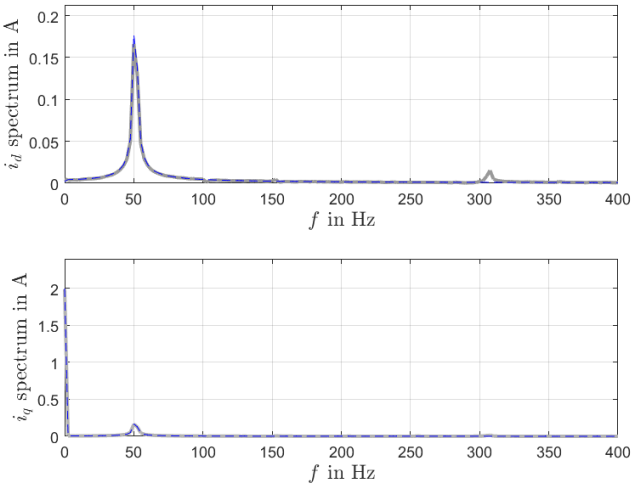

Fig. 11. FFT spectra of the experimental i_d and i_q currents (grey lines) and the model results (blue lines): load of 2.3 Nm; speed of 1000 rpm; (k_1, k_2, k_3)=(1, 1, 1); $(\Delta_1, \Delta_2, \Delta_3)$=(0.3, -0.4, 0.5)A.

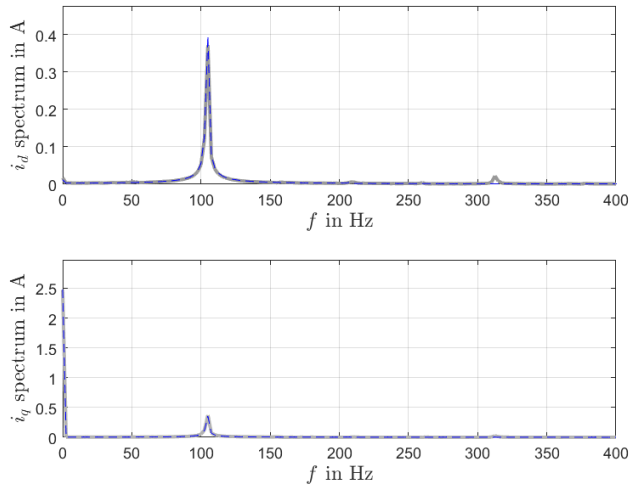

Fig. 13. FFT spectra of the experimental i_d and i_q currents (grey lines) and the model results (blue lines): load of 2.3 Nm; speed of 1000 rpm; current sensors gains (k_1, k_2, k_3)=(1, 0.5, 1); $(\Delta_1, \Delta_2, \Delta_3)$=(0, 0, 0)A.

where $\mathbf{I}$ is identity matrix, it yields:

$$\frac{\partial(\mathbf{A}')^{-1}}{\partial p_i} = (\mathbf{A}')^{-1}\frac{\partial \mathbf{A}'}{\partial p_i}(\mathbf{A}')^{-1} \tag{42}$$

which allows to express the partial derivative of the vector $\mathbf{x}$ as a function of the derivative of the matrix $\mathbf{A}'$:

$$\frac{\partial \mathbf{x}}{\partial p_i} = (\mathbf{A}')^{-1}\frac{\partial \mathbf{A}'}{\partial p_i}(\mathbf{A}')^{-1}\mathbf{b}' + (\mathbf{A}')^{-1}\frac{\partial \mathbf{b}'}{\partial p_i} \tag{43}$$

Taking into account these results, it is possible to carry out the parameter sensitivity analysis of the amplitude of the generic h^{th} harmonic of $d-$ and $q-$axis currents, defined as

$$i_{\mathrm{d},h} = \sqrt{a_{\mathrm{d},h}^2 + b_{\mathrm{d},h}^2} \tag{44}$$

and:

$$i_{\mathrm{q},h} = \sqrt{a_{\mathrm{q},h}^2 + b_{\mathrm{q},h}^2} \tag{45}$$

respectively.

Using the control and motor parameters reported in Table I and assuming $n = 6$ for the modeling approach, the results of the sensitivity analysis of the harmonics' amplitudes to resistance and inductance variations have been evaluated as a function of the speed, for different values of the load torque and of the current sensor faults. As an example, Figs. 14 and 15, show the results obtained in the case of 1.15 Nm load torque, phase current sensors' gains $(k_1, k_2, k_3) = (1, 0.5, 1)$, and phase current sensors' offsets $(\Delta_1, \Delta_2, \Delta_3) = (0.3, -0.4, 0.5)$A. The results highlight the robustness of the model to the variations of resistance and inductance at different motor speed. In fact, in the considered cases, the influence of resistance and inductance variations on the calculated values of the harmonics' amplitudes of the direct

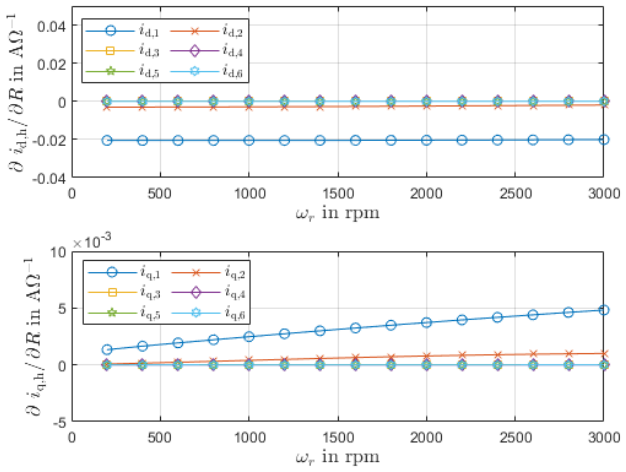

Fig. 14. Sensitivity analysis with respect to the stator resistance variations of the amplitude of the h^{th} harmonics of i_d and i_q currents: 1.15 Nm load torque; $(k_1, k_2, k_3) = (1, 0.5, 1)$; $(\Delta_1, \Delta_2, \Delta_3) = (0.3, -0.4, 0.5)$A.

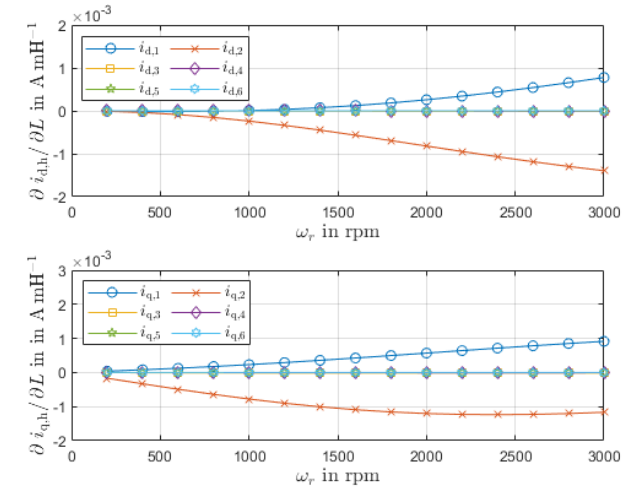

Fig. 15. Sensitivity analysis with respect to the stator inductance variations of the amplitude of the h^{th} harmonics of i_d and i_q currents: 1.15 Nm load torque; $(k_1, k_2, k_3) = (1, 0.5, 1)$; $(\Delta_1, \Delta_2, \Delta_3) = (0.3, -0.4, 0.5)$A.

and quadrature axis currents is very small. This is an important result, especially in the light of the unavoidable variations of motor parameters during the drive operations because of the temperature variations and of magnetic circuit saturation.

VIII. Conclusion

Experimental results and sensitivity analysis to parameter variations confirm the validity of the proposed closed-form analytical modeling approach of the current signature of a surface-mounted PMSM drive, controlled by means of FOC strategy, when a fault occurs in one or more phase current sensors. Both DC offset and gain fault for all current sensors have been taken into account, as well as the control loop gains. The analytical solution of the model requires the solution of an overdetermined system of equations, which has been solved by means of a new methodology which is alternative to the classical one based on the Moore-Penrose pseudoinverse matrix. The proposed modeling approach is based on the analytical expression of the reference values of the motor supply voltages as a function of the measured currents, of the speed and of the reference currents of the control loop, and on the steady state analytical solution of the differential equations which express the mathematical model of the motor. All control strategies which allow satisfying the above conditions are eligible for the application of the proposed modeling approach. The future research direction consists in using the results of this paper to set up an algorithm that, starting from the current signature, is able to get a fast and effective detection, isolation and estimation of current sensor faults in PMSM drives due to both DC offset and gain faults.

Appendix

The analytical expressions of the functions $f_{\mathrm{d},k}$, $g_{\mathrm{d},k}$, $f_{\mathrm{q},k}$ and $g_{\mathrm{q},k}$, for $k \in \{2, \ldots, n\}$, are

$$\begin{aligned}
f_{\mathrm{d},k} = {} & 0.5[p\omega_{\mathrm{r}}k(rk_{\mathrm{pd}} - p\omega_{\mathrm{r}}Lq) + qk_{\mathrm{id}}]\, a_{\mathrm{d},k-2} + \\
& + 0.5[p\omega_{\mathrm{r}}k(qk_{\mathrm{pd}} + p\omega_{\mathrm{r}}Lr) - rk_{\mathrm{id}}]\, b_{\mathrm{d},k-2} + \\
& + 0.5[p\omega_{\mathrm{r}}k(-qk_{\mathrm{pd}} - p\omega_{\mathrm{r}}Lr) + rk_{\mathrm{id}}]\, a_{\mathrm{q},k-2} + \\
& + 0.5[p\omega_{\mathrm{r}}k(rk_{\mathrm{pd}} - p\omega_{\mathrm{r}}Lq) + qk_{\mathrm{id}}]\, b_{\mathrm{q},k-2} + \\
& + (-p^2\omega_{\mathrm{r}}^2Lk^2 + sk_{\mathrm{id}})a_{\mathrm{d},k} + p\omega_{\mathrm{r}}k\big(R + sk_{\mathrm{pd}}\big)b_{\mathrm{d},k} + \\
& + p^2\omega_{\mathrm{r}}^2Lk(s-1)\, b_{\mathrm{q},k} + \\
& + 0.5[p\omega_{\mathrm{r}}k(-rk_{\mathrm{pd}} + p\omega_{\mathrm{r}}Lq) + qk_{\mathrm{id}}]\, a_{\mathrm{d},k+2} + \\
& + 0.5[p\omega_{\mathrm{r}}k(qk_{\mathrm{pd}} + p\omega_{\mathrm{r}}Lr) + rk_{\mathrm{id}}]\, b_{\mathrm{d},k+2} + \\
& + 0.5[p\omega_{\mathrm{r}}k(qk_{\mathrm{pd}} + p\omega_{\mathrm{r}}Lr) + rk_{\mathrm{id}}]\, a_{\mathrm{q},k+2} + \\
& + 0.5[p\omega_{\mathrm{r}}k(rk_{\mathrm{pd}} - p\omega_{\mathrm{r}}Lq) - qk_{\mathrm{id}}]\, b_{\mathrm{q},k+2}
\end{aligned} \tag{46}$$

$$\begin{aligned}
g_{\mathrm{d},k} = {} & 0.5[p\omega_{\mathrm{r}}k(-qk_{\mathrm{pd}} - p\omega_{\mathrm{r}}Lr) + rk_{\mathrm{id}}]\, a_{\mathrm{d},k-2} + \\
& + 0.5[p\omega_{\mathrm{r}}k(rk_{\mathrm{pd}} - p\omega_{\mathrm{r}}Lq) + qk_{\mathrm{id}}]\, b_{\mathrm{d},k-2} + \\
& + 0.5[p\omega_{\mathrm{r}}k(-rk_{\mathrm{pd}} + p\omega_{\mathrm{r}}Lq) - qk_{\mathrm{id}}]\, a_{\mathrm{q},k-2} + \\
& + 0.5[p\omega_{\mathrm{r}}k(-qk_{\mathrm{pd}} - p\omega_{\mathrm{r}}Lr) + rk_{\mathrm{id}}]\, b_{\mathrm{q},k-2} + \\
& - p\omega_{\mathrm{r}}k\big(R + sk_{\mathrm{pd}}\big)a_{\mathrm{d},k} + (-p^2\omega_{\mathrm{r}}^2Lk^2 + sk_{\mathrm{id}})b_{\mathrm{d},k} + \\
& + p^2\omega_{\mathrm{r}}^2Lk(1-s)\, a_{\mathrm{q},k} + \\
& + 0.5[p\omega_{\mathrm{r}}k(-qk_{\mathrm{pd}} - p\omega_{\mathrm{r}}Lr) - rk_{\mathrm{id}}]\, a_{\mathrm{d},k+2} + \\
& + 0.5[p\omega_{\mathrm{r}}k(-rk_{\mathrm{pd}} + p\omega_{\mathrm{r}}Lq) + qk_{\mathrm{id}}]\, b_{\mathrm{d},k+2} + \\
& + 0.5[p\omega_{\mathrm{r}}k(-rk_{\mathrm{pd}} + p\omega_{\mathrm{r}}Lq) + qk_{\mathrm{id}}]\, a_{\mathrm{q},k+2} + \\
& + 0.5[p\omega_{\mathrm{r}}k(qk_{\mathrm{pd}} + p\omega_{\mathrm{r}}Lr) + rk_{\mathrm{id}}]\, b_{\mathrm{q},k+2}
\end{aligned} \tag{47}$$

$$\begin{aligned}
f_{\mathrm{q},k} = {} & 0.5[p\omega_{\mathrm{r}}k(-qk_{\mathrm{pq}} - p\omega_{\mathrm{r}}Lr) + rk_{\mathrm{iq}}]\, a_{\mathrm{d},k-2} + \\
& + 0.5[p\omega_{\mathrm{r}}k(rk_{\mathrm{pq}} - p\omega_{\mathrm{r}}Lq) + qk_{\mathrm{iq}}]\, b_{\mathrm{d},k-2} + \\
& + 0.5[p\omega_{\mathrm{r}}k(-rk_{\mathrm{pq}} + p\omega_{\mathrm{r}}Lq) - qk_{\mathrm{iq}}]\, a_{\mathrm{q},k-2} + \\
& + 0.5[p\omega_{\mathrm{r}}k(-qk_{\mathrm{pq}} - p\omega_{\mathrm{r}}Lr) + rk_{\mathrm{iq}}]\, b_{\mathrm{q},k-2} + \\
& - p^2\omega_{\mathrm{r}}^2Lk(s-1)\, b_{\mathrm{d},k} + \\
& + (-p^2\omega_{\mathrm{r}}^2Lk^2 + sk_{\mathrm{iq}})a_{\mathrm{q},k} + p\omega_{\mathrm{r}}k\big(R + sk_{\mathrm{pq}}\big)b_{\mathrm{q},k} + \\
& + 0.5[p\omega_{\mathrm{r}}k(qk_{\mathrm{pq}} + p\omega_{\mathrm{r}}Lr) + rk_{\mathrm{iq}}]\, a_{\mathrm{d},k+2} + \\
& + 0.5[p\omega_{\mathrm{r}}k(rk_{\mathrm{pq}} - p\omega_{\mathrm{r}}Lq) - qk_{\mathrm{iq}}]\, b_{\mathrm{d},k+2} + \\
& + 0.5[p\omega_{\mathrm{r}}k(rk_{\mathrm{pq}} - p\omega_{\mathrm{r}}Lq) - qk_{\mathrm{iq}}]\, a_{\mathrm{q},k+2} + \\
& + 0.5[p\omega_{\mathrm{r}}k(-qk_{\mathrm{pq}} - p\omega_{\mathrm{r}}Lr) - rk_{\mathrm{iq}}]\, b_{\mathrm{q},k+2}
\end{aligned} \tag{48}$$

$$
\begin{aligned}
g_{\mathrm{q},k} = {} & 0.5[p\omega_{\mathrm{r}}k(-rk_{\mathrm{pq}} + p\omega_{\mathrm{r}}Lq) - qk_{\mathrm{iq}}]\, a_{\mathrm{d},k-2} + \\
& + 0.5[p\omega_{\mathrm{r}}k(-qk_{\mathrm{pq}} - p\omega_{\mathrm{r}}Lr) + rk_{\mathrm{iq}}]\, b_{\mathrm{d},k-2} + \\
& + 0.5[p\omega_{\mathrm{r}}k(qk_{\mathrm{pq}} + p\omega_{\mathrm{r}}Lr) - rk_{\mathrm{iq}}]\, a_{\mathrm{q},k-2} + \\
& + 0.5[p\omega_{\mathrm{r}}k(-rk_{\mathrm{pq}} + p\omega_{\mathrm{r}}Lq) - qk_{\mathrm{iq}}]\, b_{\mathrm{q},k-2} + \\
& + p^2\omega_{\mathrm{r}}^2Lk(s-1)\, a_{\mathrm{d},k} + \\
& - p\omega_{\mathrm{r}}k\big(R + sk_{\mathrm{pq}}\big)a_{\mathrm{q},k} + (-p^2\omega_{\mathrm{r}}^2Lk^2 + sk_{\mathrm{iq}})b_{\mathrm{q},k} + \\
& + 0.5[p\omega_{\mathrm{r}}k(-rk_{\mathrm{pq}} + p\omega_{\mathrm{r}}Lq) + qk_{\mathrm{iq}}]\, a_{\mathrm{d},k+2} + \\
& + 0.5[p\omega_{\mathrm{r}}k(qk_{\mathrm{pq}} + p\omega_{\mathrm{r}}Lr) + rk_{\mathrm{iq}}]\, b_{\mathrm{d},k+2} + \\
& + 0.5[p\omega_{\mathrm{r}}k(qk_{\mathrm{pq}} + p\omega_{\mathrm{r}}Lr) + rk_{\mathrm{iq}}]\, a_{\mathrm{q},k+2} + \\
& + 0.5[p\omega_{\mathrm{r}}k(rk_{\mathrm{pq}} - p\omega_{\mathrm{r}}Lq) - qk_{\mathrm{iq}}]\, b_{\mathrm{q},k+2}
\end{aligned} \tag{49}
$$

Equations (46), (47), (48), (49) can also be used to determine $f_{\mathrm{d},1}$, $g_{\mathrm{d},1}$, $f_{\mathrm{q},1}$, $g_{\mathrm{q},1}$, $f_{\mathrm{d},n+2}$, $g_{\mathrm{d},n+2}$, $f_{\mathrm{q},n+2}$ and $g_{\mathrm{q},n+2}$.

In particular, $f_{\mathrm{d},1}$, $g_{\mathrm{d},1}$, $f_{\mathrm{q},1}$, $g_{\mathrm{q},1}$ are obtained from (46), (47), (48), (49), respectively, by setting equal to zero the coefficients having subscript -1 and adding the following terms

$$\text{to (46)}: \quad \delta_\alpha(-p^2\omega_{\mathrm{r}}^2L + k_{\mathrm{id}}) + \delta_\beta\, p\omega_{\mathrm{r}}k_{\mathrm{pd}} \tag{50}$$

$$\text{to (47)}: \quad -\delta_\alpha p\omega_{\mathrm{r}}k_{\mathrm{pd}} + \delta_\beta(-p^2\omega_{\mathrm{r}}^2L + k_{\mathrm{id}}) \tag{51}$$

$$\text{to (48)}: \quad -\delta_\alpha p\omega_{\mathrm{r}}k_{\mathrm{pq}} + \delta_\beta(-p^2\omega_{\mathrm{r}}^2L + k_{\mathrm{iq}}) \tag{52}$$

$$\text{to (49)}: \quad -\delta_\alpha(k_{\mathrm{iq}} - p^2\omega_{\mathrm{r}}^2L) - \delta_\beta\, p\omega_{\mathrm{r}}k_{\mathrm{pq}} \tag{53}$$

In particular, $f_{\mathrm{d},2}$, $g_{\mathrm{d},2}$, $f_{\mathrm{q},2}$, $g_{\mathrm{q},2}$ are obtained from (46), (47), (48), (49), respectively, by setting equal to zero the coefficients having subscript 0 and adding the following terms

$$
\begin{aligned}
\text{to (46)}: \quad & \big[2p\omega_{\mathrm{r}}(rk_{\mathrm{pd}} - p\omega_{\mathrm{r}}Lq) + qk_{\mathrm{id}}\big]\, c_{\mathrm{d}} + \\
& + \big[-2p\omega_{\mathrm{r}}(qk_{\mathrm{pd}} + p\omega_{\mathrm{r}}Lr) + rk_{\mathrm{id}}\big]\, c_{\mathrm{q}}
\end{aligned} \tag{54}
$$

$$
\begin{aligned}
\text{to (47)}: \quad & \big[-2p\omega_{\mathrm{r}}(qk_{\mathrm{pd}} + p\omega_{\mathrm{r}}Lr) + rk_{\mathrm{id}}\big]\, c_{\mathrm{d}} + \\
& + \big[-2p\omega_{\mathrm{r}}(rk_{\mathrm{pd}} - p\omega_{\mathrm{r}}Lq) - qk_{\mathrm{id}}\big]\, c_{\mathrm{q}}
\end{aligned} \tag{55}
$$

$$
\begin{aligned}
\text{to (48)}: \quad & \big[-2p\omega_{\mathrm{r}}(qk_{\mathrm{pq}} + p\omega_{\mathrm{r}}Lr) + rk_{\mathrm{iq}}\big]\, c_{\mathrm{d}} + \\
& \big[-2p\omega_{\mathrm{r}}(qk_{\mathrm{pq}} - p\omega_{\mathrm{r}}Lr) - rk_{\mathrm{iq}}\big]\, c_{\mathrm{q}}
\end{aligned} \tag{56}
$$

$$
\begin{aligned}
\text{to (49)}: \quad & \big[-2p\omega_{\mathrm{r}}(rk_{\mathrm{pq}} - p\omega_{\mathrm{r}}Lq) - qk_{\mathrm{iq}}\big]\, c_{\mathrm{d}} + \\
& \big[2p\omega_{\mathrm{r}}(qk_{\mathrm{pq}} + p\omega_{\mathrm{r}}Lr) - rk_{\mathrm{iq}}\big]\, c_{\mathrm{q}}
\end{aligned} \tag{57}
$$

while $f_{\mathrm{d},n+1}$, $g_{\mathrm{d},n+1}$, $f_{\mathrm{q},n+1}$, $g_{\mathrm{q},n+1}$ are simply obtained by setting equal to zero the coefficients having subscript $n+2$. Eventually, the analytical expressions of the functions $f_{\mathrm{d},0}$ and $f_{\mathrm{q},0}$ are

$$f_{\mathrm{d},0} = k_{\mathrm{id}}\big(qa_{\mathrm{d},1} + rb_{\mathrm{d},1} + ra_{\mathrm{q},1} - qb_{\mathrm{q},1} + sc_{\mathrm{d}}\big) \tag{58}$$

$$f_{\mathrm{q},0} = k_{\mathrm{iq}}\big(ra_{\mathrm{d},1} - qb_{\mathrm{d},1} - qa_{\mathrm{q},1} - rb_{\mathrm{q},1} + sc_{\mathrm{q}}\big) \tag{59}$$

REFERENCES

[1] I. Husain, B. Ozpineci, M. S. Islam, E. Gurpinar, G.-J. Su, W. Yu, S. Chowdhury, L. Xue, D. Rahman, and R. Sahu, "Electric drive technology trends, challenges, and opportunities for future electric vehicles," *Proceedings of the IEEE*, vol. 109, no. 6, pp. 1039–1059, 2021.

[2] K. Ni, Y. Liu, Z. Mei, T. Wu, Y. Hu, H. Wen, and Y. Wang, "Electrical and electronic technologies in more-electric aircraft: A review," *IEEE Access*, vol. 7, pp. 76 145–76 166, 2019.

[3] Y. Chen, S. Liang, W. Li, H. Liang, and C. Wang, "Faults and diagnosis methods of permanent magnet synchronous motors: A review," *Applied Sciences*, vol. 9, no. 10, p. 2116, 2019.

[4] M. El Hachemi Benbouzid, "A review of induction motors signature analysis as a medium for faults detection," *IEEE Transactions on Industrial Electronics*, vol. 47, no. 5, pp. 984–993, 2000.

[5] G. B. Kliman and J. Stein, "Methods of motor current signature analysis," *Electrical Machines and Power Systems*, vol. 20, no. 5, pp. 463–474, 1992.

[6] C. P. Salomon, W. C. Santana, G. Lambert-Torres, L. E. B. da Silva, E. L. Bonaldi, L. E. d. L. de Oliveira, J. G. B. da Silva, A. L. Pellicel, G. C. Figueiredo, and M. A. A. Lopes, "Discrimination of synchronous machines rotor faults in electrical signature analysis based on symmetrical components," *IEEE Transactions on Industry Applications*, vol. 53, no. 3, pp. 3146–3155, 2016.

[7] J. Hang, J. Zhang, M. Cheng, and S. Ding, "Detection and discrimination of open-phase fault in permanent magnet synchronous motor drive system," *IEEE Transactions on Power Electronics*, vol. 31, no. 7, pp. 4697–4709, 2016.

[8] J.-C. Urresty, J.-R. Riba, and L. Romeral, "Diagnosis of interturn faults in pmsms operating under nonstationary conditions by applying order tracking filtering," *IEEE Transactions on Power Electronics*, vol. 28, no. 1, pp. 507–515, 2013.

[9] J. Rosero, L. Romeral, J. Cusido, A. Garcia, and J. Ortega, "On the short-circuiting fault detection in a pmsm by means of stator current transformations," in *2007 IEEE Power Electronics Specialists Conference*, 2007, pp. 1936–1941.

[10] M. A. Mazzoletti, G. R. Bossio, C. H. De Angelo, and D. R. Espinoza-Trejo, "A model-based strategy for interturn short-circuit fault diagnosis in pmsm," *IEEE Transactions on Industrial Electronics*, vol. 64, no. 9, pp. 7218–7228, 2017.

[11] Y. Qi, E. Bostanci, V. Gurusamy, and B. Akin, "A comprehensive analysis of short-circuit current behavior in pmsm interturn short-circuit faults," *IEEE Transactions on Power Electronics*, vol. 33, no. 12, pp. 10 784–10 793, 2018.

[12] G. Forstner, A. Kugi, and W. Kemmetmüller, "A magnetic equivalent circuit based modeling framework for electric motors applied to a pmsm with winding short circuit," *IEEE Transactions on Power Electronics*, vol. 35, no. 11, pp. 12 285–12 295, 2020.

[13] A. G. Espinosa, J. A. Rosero, J. Cusidó, L. Romeral, and J. A. Ortega, "Fault detection by means of hilbert–huang transform of the stator current in a pmsm with demagnetization," *IEEE Transactions on Energy Conversion*, vol. 25, no. 2, pp. 312–318, 2010.

[14] J. C. Urresty, J. R. Riba, and L. Romeral, "Influence of the stator windings configuration in the currents and zero-sequence voltage harmonics in permanent magnet synchronous motors with demagnetization faults," *IEEE Transactions on Magnetics*, vol. 49, no. 8, pp. 4885–4893, 2013.

[15] J. Faiz and E. Mazaheri-Tehrani, "Demagnetization modeling and fault diagnosing techniques in permanent magnet machines under stationary and nonstationary conditions: An overview," *IEEE Transactions on Industry Applications*, vol. 53, no. 3, pp. 2772–2785, 2016.

[16] J. Hang, J. Zhang, M. Cheng, and Z. Wang, "Fault diagnosis of mechanical unbalance for permanent magnet synchronous motor drive system under nonstationary condition," in *2013 IEEE Energy Conversion Congress and Exposition*, 2013, pp. 3556–3562.

[17] W. le Roux, R. G. Harley, and T. G. Habetler, "Detecting rotor faults in low power permanent magnet synchronous machines," *IEEE Transactions on Power Electronics*, vol. 22, no. 1, pp. 322–328, 2007.

[18] B. M. Ebrahimi, M. Javan Roshtkhari, J. Faiz, and S. V. Khatami, "Advanced eccentricity fault recognition in permanent magnet synchronous motors using stator current signature analysis," *IEEE Transactions on Industrial Electronics*, vol. 61, no. 4, pp. 2041–2052, 2014.

[19] G. A. Skarmoutsos, K. N. Gyftakis, and M. Mueller, "Analytical prediction of the mcsa signatures under dynamic eccentricity in pm machines with concentrated non-overlapping windings," *IEEE Transactions on Energy Conversion*, vol. 37, no. 2, pp. 1011–1019, 2022.

[20] S. K. Kommuri, S. B. Lee, and K. C. Veluvolu, "Robust sensors-fault-tolerance with sliding mode estimation and control for pmsm drives," *IEEE/ASME Transactions on Mechatronics*, vol. 23, no. 1, pp. 17–28, 2017.
[21] G. Huang, J. She, E. F. Fukushima, C. Zhang, and J. He, "Robust reconstruction of current sensor faults for pmsm drives in the presence of disturbances," *IEEE/ASME Transactions on Mechatronics*, vol. 24, no. 6, pp. 2919–2930, 2019.
[22] C. Attaianese, M. D'Arpino, M. Di Monaco, and L. P. Di Noia, "Model-based detection and estimation of dc offset of phase current sensors for field oriented pmsm drives," *IEEE Transactions on Industrial Electronics*, 2022.
[23] C. Attaianese, M. D'Arpino, M. Di Monaco, and L. P. Di Noia, "Modeling and detection of phase current sensor gain faults in pmsm drives," *IEEE Access*, vol. 10, pp. 80 106–80 118, 2022.
[24] B. K. Bose, "Power electronics and ac drives," *Englewood Cliffs*, 1986.
[25] W. E. Boyce, R. C. DiPrima, and D. B. Meade, *Elementary differential equations and boundary value problems*. John Wiley & Sons, 2021.
[26] A. Cichocki and S.-i. Amari, *Adaptive Blind Signal and Image Processing - Learning Algorithms and Applications*. John Wiley & Sons, 2003.

Ciro Attaianese received the Ph.D. in Electrical Engineering from the University of Naples Federico II, Italy, 1989. He joined the University of Cassino and Southern Lazio as Associate Professor of Electrical Machines, Power Electronics and Electric Drives in 1992. He became full professor in 1999. In 2019, he joined the University of Naples Federico II. He is founder of three startups operating in the field of power electronics and e-mobility. His current research interests include electrical machines and power converters modelling, electrical drives and applications of microprocessors to their control, renewable energy, electrification of mobility.

Matilde D'Arpino received the Ph.D. degree in 'Systems, technologies, and devices for movement and health' from the University of Cassino, Italy, in 2014, respectively. From 2016 to 2022, she has been a researcher at the Ohio State University Center for Automotive Research, Columbus, OH, USA. Currently, she is Research Assistant Professor with the Department of Mechanical and Aerospace Engineering at the Ohio State University. Her research interests include power converters and energy management controls for multi-source power systems (e.g. microgrids, hybrid vehicles, hybrid aircraft), testing, modeling, design, control and diagnostic of energy storage systems.

Mauro Di Monaco was born in Cassino, Italy, on October 11, 1981. He received the B.Sc. in electrical engineering and the Ph.D. degree from the University of Cassino, Italy, in 2006 and 2010, respectively. Since 2010, he has been a Researcher with the Laboratory of Industrial Automation, University of Cassino and South Lazio, Italy. His research activities mainly include the study and the implementation of new optimization algorithms and modulation techniques for multi-level and multi-source power converters in the fields of renewable energy and e-mobility, new powertrain architectures and control techniques for electric vehicles.

Luigi Pio Di Noia received the M.S. and Ph.D. degrees in electrical engineering from the University of Naples Federico II, Napoli, Italy, in 2011 and 2015, respectively. Since 2018, he has been a research fellow of Electrical Machines, Power Electronics and Electric Drives. His research interests include the design and control of electrical machines and drives for electrification of traction and propulsion, fault diagnosis and prognostic.